IOPscience iopscience.iop.org

Home Search Collections Journals About Contact us My IOPscience

Quadrupole shape dynamics from the viewpoint of a theory of large-amplitude collective motion

This content has been downloaded from IOPscience. Please scroll down to see the full text.

2014 Phys. Scr. 89 054020

(http://iopscience.iop.org/1402-4896/89/5/054020)

View the table of contents for this issue, or go to the journal homepage for more

Download details:
This content was downloaded by: matsuyanagi
IP Address: 120.74.165.137
This content was downloaded on 01/05/2014 at 12:49

Please note that terms and conditions apply.

IOP Publishing | Royal Swedish Academy of Sciences Physica Scripta

Phys. Scr. **89** (2014) 054020 (6pp) doi:10.1088/0031-8949/89/5/054020

Quadrupole shape dynamics from the viewpoint of a theory of large-amplitude collective motion

M Matsuo[1], N Hinohara[2], K Sato[3], K Matsuyanagi[3], T Nakatsukasa[3] and K Yoshida[4]

[1] Department of Physics, Faculty of Science, Niigata University, Niigata 950-2181, Japan
[2] Department of Physics and Astronomy, University of North Carolina, Chapel Hill, NC 27599-3255, USA
[3] RIKEN Nishina Center, Wako 351-0198, Japan
[4] Graduate School of Science and Technology, Niigata University, Niigata 950-2181, Japan

E-mail: matsuo@nt.sc.niigata-u.ac.jp

Received 18 November 2013, revised 27 December 2013
Accepted for publication 27 December 2013
Published 29 April 2014

Abstract

Low-lying quadrupole shape dynamics is a typical manifestation of large-amplitude collective motion in finite nuclei. To describe the dynamics on a microscopic foundation, we have formulated a consistent scheme in which the Bohr collective Hamiltonian for the five-dimensional quadrupole shape variables is derived on the basis of the time-dependent Hartree–Fock–Bogoliubov theory. It enables us to incorporate the Thouless–Valatin effect on the shape inertial functions, which has been neglected in previous microscopic Bohr Hamiltonian approaches. Quantitative successes are illustrated for the low-lying spectra in ^{68}Se, $^{30-34}$Mg and $^{58-64}$Cr, which display shape-coexistence, shape-mixing and shape-transitional behavior.

Keywords: quadrupole shape motion, microscopic Bohr Hamiltonian, adiabatic selfconsistent collective coordinate method, local quasiparticle random phase approximation

(Some figures may appear in colour only in the online journal)

1. Introduction

Recent nuclear structure studies have developed significantly in moving far from the stability line as they are boosted by the RI beam facilities and the advanced detector technologies. Low-lying quadrupole collectivity is one of the highlights, as characteristic spectra suggesting onset of large deformation and coexistence of different shapes are often observed in new regions of the experimental studies. A typical example is neutron-rich nuclei around ^{32}Mg, in which the lowering of the 2^+ energy and the increase of $B(E2)$ with increase of the neutron number indicate unusual onset of quadrupole collectivity at the magic number $N = 20$. Recent identification of the second 0^+ states at very low excitation energy $\sim$1 MeV [1] poses further questions on the nature of this state: for instance, whether it suggests the coexistence of spherical and prolately deformed states or not. Such a new region of quadrupole collectivity is also found in neutron-rich Cr isotopes.

The theoretical description of excitation spectra associated with the shape coexistence and the shape transition is not a simple issue. It is customary to consider the deformation energy surface by considering mean-field states with various shapes in the β–γ plane. However, the deformed states can rotate and the deformation may evolve from one local minimum to others. One needs to describe this large-amplitude dynamics. Bohr's five-dimensional quadrupole coordinates $a_{2\mu}\,(\mu = -2, -1, 0, 1, 2)$, or equivalently the β–γ variables and the three Euler angles [2, 3] are suitable degrees of freedom for this purpose, but one then has to construct the collective Hamiltonian on the basis of the nucleon many-body

 © 2014 The Royal Swedish Academy of Sciences Printed in the UK

Hamiltonian. This is a central problem in this collective Hamiltonian approach, and several theories have been developed.

The Bohr collective Hamiltonian consists of the collective potential $V(\beta, \gamma)$ and the kinetic energy term related to the rotational and shape degrees of freedom, represented by the three moments of inertia $\mathcal{J}_k(\beta, \gamma)$, with $k = 1, 2, 3$ being the principal axes of the deformation, and the three shape inertial functions $D_{\beta\beta}(\beta, \gamma)$, $D_{\gamma\gamma}(\beta, \gamma)$, and $D_{\beta\gamma}(\beta, \gamma)$, which govern the kinetic energy originating from the shape motion. In previous theories of the microscopic Bohr Hamiltonian [4–10], however, the Inglis–Belyaev cranking approximation is often adopted to evaluate the inertial functions, i.e. the velocity-dependent and time-odd mean fields induced by the collective motion are neglected. This leads to an underestimate of the inertial functions, and consequently to an overall stretching of excitation spectra compared with the experimental observation [5, 10]. If one includes the time-odd effect (the Thouless–Valatin effect) on the rotational moments of inertia, the description of the yrast spectra is improved [11–13], but leaves the problem in the yrare states such as the second 0^+ state. Clearly one should also consider the Thouless–Valatin effect on the shape inertial functions.

We have developed a microscopic theory of the quadrupole collective dynamics which satisfies the above mentioned requirements [14–19]. It is based on a general theory of the large-amplitude collective motion, called the self-consistent collective coordinate (SCC) method [20, 21]. The SCC method starts with the time-dependent Hartree–Fock or time-dependent Hartree–Fock–Bogoliubov (TDHFB) theory, that is powerful to describe many-body time-evolution of nuclei, including large-amplitude motions such as a low-energy heavy-ion collision [22, 23]. It provides a scheme to extract the collective submanifold from the whole space of the TDHFB state vectors, and hence define consistently collective coordinates and a collective Hamiltonian associated with the collective submanifold. Applying this method to the quadrupole shape dynamics, we succeeded in constructing the Bohr Hamiltonian from the microscopic many-body Hamiltonian [14]. After briefly reviewing this theoretical scheme, we illustrate how the theory solves the problem of the stretched spectra, and works well for quantitative description of the quadrupole shape dynamics.

2. Adiabatic SCC method: theoretical backbone

The time-evolution of the TDHFB state vector (a generalized determinantal state) $|\phi(t)\rangle$ is given by the time-dependent variational principle

$$\delta \langle \phi(t)| \; i\frac{\partial}{\partial t} - \hat{H} \; |\phi(t)\rangle = 0. \tag{1}$$

The SCC method [20] then assumes that the collective motion under consideration corresponds to a subset of solutions of this equation, and that there exist collective coordinates and momenta $(q_i, p_i)(i = 1 - M)$ that describe the collective motion. This means that the time-evolution of the state vector is described via the time-evolution of (q_i, p_i), which parametrize the TDHFB state vectors, i.e. $|\phi(t)\rangle = |\phi(q(t), p(t))\rangle$. The parametrized TDHFB state vectors $\{|\phi(q, p)\rangle\}$ are called the collective submanifold. The time-evolution is governed by the collective Hamiltonian $\mathcal{H}_{\rm coll}(q, p) \equiv \langle \phi(q, p)| \; \hat{H} \; |\phi(q, p)\rangle$ and the canonical equation of motion $\frac{dq_i}{dt} = \frac{\partial \mathcal{H}_{\rm coll}}{\partial p_i}$, $\frac{dp_i}{dt} = -\frac{\partial \mathcal{H}_{\rm coll}}{\partial q_i}$. Then, the time-dependent variational principle equation (1) is transformed to the equation of the collective submanifold

$$\delta \langle \phi(q, p)| \left(\frac{\partial \mathcal{H}_{\rm coll}}{\partial p_i} \hat{P}^i + \frac{\partial \mathcal{H}_{\rm coll}}{\partial q_i} \hat{Q}^i \right) - \hat{H} \; |\phi(q, p)\rangle = 0, \tag{2}$$

where $\hat{P}^i$ and $\hat{Q}^i$ are displacement operators defined by $\hat{P}^i \; |\phi(q, p)\rangle = i\frac{\partial}{\partial q_i} \; |\phi(q, p)\rangle$ and $\hat{Q}^i \; |\phi(q, p)\rangle = -i\frac{\partial}{\partial p_i} \; |\phi(q, p)\rangle$, and they are one-body operators thanks to the Thouless theorem. Equation (2) is selfcontained.

To solve the equation, we introduce an expansion with respect to the collective momenta p, assuming that the collective Hamiltonian has a natural form

$$\mathcal{H}_{\rm coll}(q, p) = \frac{1}{2} D(q)^{-1}_{ij} p_i p_j + V(q), \tag{3}$$

consisting of the kinetic energy of the collective motion with the inertial function $D(q)_{ij}$ and the collective potential function $V(q)$. The state vector is expressed as $|\phi(q, p)\rangle = \exp\left(ip_i \hat{Q}^i(q)\right) |\phi(q)\rangle$ using the Thouless theorem. Expanding the equation of collective submanifold (2) with respect to the powers of p, we obtain the following set of equations: (i) *the moving-frame HFB equation*

$$\delta \langle \phi(q)| \; \hat{H} - \frac{\partial V}{\partial q_i} \hat{Q}^i(q) \; |\phi(q)\rangle = 0, \tag{4}$$

(ii) *the moving-frame QRPA equation*

$$\begin{aligned} &\delta \langle \phi(q)| \left[\hat{H}_M(q), \hat{Q}^i(q) \right] - D(q)^{-1}_{ij} \hat{P}^j(q) \Big/ i \; |\phi(q)\rangle = 0, \\ &\delta \langle \phi(q)| \left[\hat{H}_M(q), \hat{P}^i(q) \right] - iC_{ij}(q) \hat{Q}^j(q) \\ &\quad - \frac{\partial V}{\partial q_j} \Delta \hat{Q}^i_j(q) \; |\phi(q)\rangle = 0, \end{aligned} \tag{5}$$

together with the definitions of the collective potential $V(q) = \langle \phi(q)| \; \hat{H} \; |\phi(q)\rangle$, the collective inertial function $D(q)^{-1}_{ij} = -\langle \phi(q)| \left[\left[\hat{H}, \hat{Q}^i(q) \right], \hat{Q}^j(q) \right] |\phi(q)\rangle$, and the

moving-frame Hamiltonian $\hat{H}_M(q) = \hat{H} - \frac{\partial V}{\partial q_i}\hat{Q}^i(q)$. Apart from the curvature term $\Delta\hat{Q}(q)$, equation (5) is similar to the QRPA equation determining a normal mode. Note that $\hat{Q}^i(q)$ also plays the role of a constraining operator in the moving-frame HFB equation, and hence the two equations are coupled. These are basic equations of the adiabatic SCC (ASCC) method [21]. The ASCC method is a natural extension of the RPA theory, with which one can extract normal modes of small amplitude oscillation.

3. CHFB plus local QRPA approach: a practical implementation

Our scheme to derive the Bohr collective Hamiltonian is a practical and approximate implementation of the ASCC method [14]. We first perform a standard constrained Hartree–Fock–Bogoliubov (CHFB) calculation to obtain mean-field states $\left|\phi_{\rm CHFB}(\beta,\gamma)\right\rangle$ with various quadrupole deformations in the β–γ plane. We assume that the collective submanifold states $|\phi(q)\rangle$ have a one-to-one mapping to the CHFB states $\left|\phi_{\rm CHFB}(\beta,\gamma)\right\rangle$ by a coordinate transformation. The collective potential is then the deformation energy of the CHFB states $V(\beta,\gamma) = \left\langle\phi_{\rm CHFB}(\beta,\gamma)\right|\hat{H}\left|\phi_{\rm CHFB}(\beta,\gamma)\right\rangle$. For the moving-frame QRPA equation (5), we neglect the curvature term $\Delta\hat{Q}$ and replace $\hat{H}_M(q)$ with the constrained Hamiltonian $\hat{H}_{\rm CHFB}$, and we solve

$$\delta\left\langle\phi_{\rm CHFB}(\beta,\gamma)\right|\left[\hat{H}_{\rm CHFB},\hat{Q}^i\right] - D_i^{-1}\hat{P}^i/i\left|\phi_{\rm CHFB}(\beta,\gamma)\right\rangle = 0,$$
$$\delta\left\langle\phi_{\rm CHFB}(\beta,\gamma)\right|\left[\hat{H}_{\rm CHFB},\hat{P}^i/i\right] - C_i\hat{Q}^i\left|\phi_{\rm CHFB}(\beta,\gamma)\right\rangle = 0. \quad (6)$$

We call these local QRPA (LQRPA) equations. They determine the displacement operators $\hat{Q}^i$ and $\hat{P}^i$, and hence the vibrational collective coordinates (q_i, p_i), which are orthonormal locally at each (β,γ) point. (C_{ij} and D_{ij}^{-1} are diagonal then, and for simplicity we often choose the scale satisfying $D_i = 1$.) Among various QRPA solutions we select two which are most effective to change the quadrupole deformations. The collective coordinates of the normal modes (q_i, p_i) $(i = 1, 2)$ can be related to the Bohr quadrupole shape variables $a_{20} = c\left\langle\hat{Q}_{20}\right\rangle$, $a_{22} = c\left\langle\hat{Q}_{22}\right\rangle$ via

$$\frac{\partial a_{2m}}{\partial q_i} = c\left\langle\phi_{\rm CHFB}(\beta,\gamma)\right|\left[\hat{Q}_{2m},\hat{P}^i/i\right]\left|\phi_{\rm CHFB}(\beta,\gamma)\right\rangle. \quad (7)$$

The vibrational kinetic energy $T_{\rm vib} = \left(p_1^2 + p_2^2\right)/2 = \left(\dot{q}_1^2 + \dot{q}_2^2\right)/2$ is then expressed in the Bohr coordinates as

$$T_{\rm vib} = \frac{1}{2}\sum_{mm'=0,2} M_{mm'}\dot{a}_{2m}\dot{a}_{2m'}$$
$$= \frac{1}{2}D_{\beta\beta}(\beta,\gamma)\dot{\beta}\dot{\beta} + D_{\beta\gamma}(\beta,\gamma)\dot{\beta}\dot{\gamma} + \frac{1}{2}D_{\gamma\gamma}(\beta,\gamma)\dot{\gamma}\dot{\gamma}, \quad (8)$$

with

$$M_{mm'} = \sum_{i=1,2}\frac{\partial q^i}{\partial a_{2m}}\frac{\partial q^i}{\partial a_{2m'}}, \quad (9)$$

and the inertial functions $D_{\beta\beta}$, $D_{\beta\gamma}$ and $D_{\gamma\gamma}$ are derived from $M_{mm'}$ by a straight variable transformation from (a_{20}, a_{22}) to (β,γ). We also calculate the rotational moments of inertia by using the local QRPA equation

$$\delta\left\langle\phi_{\rm CHFB}(\beta,\gamma)\right|\left[\hat{H}_{\rm CHFB},\hat{\Theta}_k\right] - \mathcal{J}_k^{-1}\hat{I}_k/i\left|\phi_{\rm CHFB}(\beta,\gamma)\right\rangle = 0, \quad (10)$$

$(k = 1, 2, 3)$ for the rotation around the three principal axes, and obtain the rotational kinetic energy $T_{\rm rot} = \frac{1}{2}\sum_k \mathcal{J}_k(\beta,\gamma)\omega_k^2$.

We do not neglect any residual interactions in solving the LQRPA equations; i.e. we take into account all the induced fields, including the time-odd ones, associated with the collective rotations and the β–γ shape motions. The Thouless–Valatin effects are thus taken into account for all the inertial functions $\mathcal{J}_x$, $\mathcal{J}_y$, $\mathcal{J}_z$, $D_{\beta\beta}$, $D_{\beta\gamma}$ and $D_{\gamma\gamma}$. If the residual interactions were neglected in solving equations (6) and (10), the approximation would lead to the Inglis–Belyaev inertial functions. Although the Thouless–Valatin effect on the rotational moments of inertia is widely known, and is taken into account in a recent approach [11–13], the systematic inclusion of the Thouless–Valatin effect on the vibrational inertia is achieved in our approach for the first time.

4. Quadrupole dynamics with the LQRPA inertial functions

In applications of the CHFB+LQRPA, we have to solve the QRPA equations for all the CHFB states with various deformations. To construct the CHFB states and the QRPA solutions, we employ the pairing plus quadrupole model. Two major shells are adopted as a model space for each of neutrons and protons. The single-particle energies, the force parameters of the monopole pairing interaction and the quadrupole–quadrupole interaction are adjusted to reproduce the results of the Skyrme–HFB calculation. The quadrupole pairing interaction is also taken into account, since it is known to bring about the Thouless–Valatin effect [24]. We use the selfconsistent strength of the quadrupole pairing, with which the Galilean invariance of the pairing interaction is recovered [24]. We first obtain the CHFB states $\left|\phi_{\rm CHFB}(\beta,\gamma)\right\rangle$ for 60×60 mesh points, discretized both for $\beta = 0 - \beta_{\rm max}$

(typically $\beta_{\max} = 0.6$) and for $\gamma = 0 - \pi/3$. The QRPA equations are then solved the same number of times.

To obtain the excitation spectra of the quadrupole dynamics, we requantize the Bohr Hamiltonian using the standard Pauli prescription:

$$\{\hat{T}_{\rm vib} + \hat{T}_{\rm rot} + V\}\Psi_{\alpha\, IM}(\beta, \gamma, \Omega) = E_{\alpha I}\Psi_{\alpha\, IM}(\beta, \gamma, \Omega). \quad (11)$$

Expressing the collective wave function $\Psi_{\alpha\, IM}(\beta, \gamma, \Omega) = \sum_K \Phi_{\alpha IK}(\beta, \gamma)\langle \Omega | IMK \rangle$ directly on the 60 × 60 mesh points in the β–γ plane, we diagonalize a Hamiltonian matrix in the mesh representation. Ω is the Euler angle, and $\langle \Omega | IMK \rangle$ is the rotational function.

4.1. Spectra in ^{68}Se and the Thouless–Valatin effect

The first application of the CHFB+LQRPA approach was performed for ^{68}Se [14], in which the experimental spectra suggest possible coexistence of oblate and prolate shapes. The calculated CHFB potential energy surface indeed shows two minima at prolate shape $\beta \sim 0.3$, $\gamma = 0$ and at oblate shape $\beta \sim 0.3$, $\gamma = \pi/3$, but the potential energy surface is soft with respect to the γ direction with an energy difference of several hundred keV and a few hundred keV barrier.

The Thouless–Valatin effect is examined by comparing the LQRPA inertia, for instance, $D_{\beta\beta}$, with the same quantity $D^{(IB)}_{\beta\beta}$ evaluated in the Inglis–Belyaev cranking approximation. We have found that the ratio $D_{\beta\beta}/D^{(IB)}_{\beta\beta}$ is typically 1.3–1.5 in a large part of the β–γ plane, where the deformation energy is not large. At larger deformation $\beta \gtrsim 0.4$ it takes values around 2. Concerning the rotational moment of inertia, the ratio $\mathcal{J}_1/\mathcal{J}^{(IB)}_1$ takes a value around 1.2–1.5 at small and modest deformation, but it decreases to ∼1.1 at large deformations. The deformation dependence is different between the LQRPA inertia and the IB inertia. Also the six inertial functions have different deformation dependences.

The Thouless–Valatin effects on the inertial functions have an impact on the excitation spectra. When we perform a calculation using the Inglis–Belyaev cranking inertia, the excitation energies of the yrast states are $E(2^+_1), E(4^+_1), E(6^+_1) = 0.991, 2.310, 3.891$ MeV, which are systematically larger than the corresponding experimental values 0.854, 1.942, 3.304 MeV by about 20%. This deficiency is improved in the CHFB+LQRPA calculation, producing $E(2^+_1), E(4^+_1), E(6^+_1) = 0.810, 1.951, 3.348$ MeV, in much better agreement with the experiment. The improvement is also achieved for the yrare states; the CHFB +LQRPA description gives the second 2^+ state at $E(2^+_2) = 1.536$ MeV, consistent with the experimental value $E(2^+_2) = 1.593$ MeV, and much better than the calculation $E(2^+_2) = 1.883$ MeV using the Inglis–Belyaev inertia.

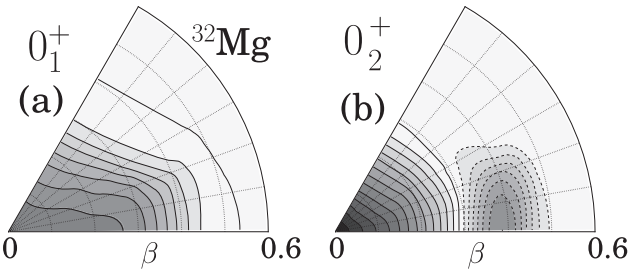

Figure 1. Vibrational wave functions $\Phi_{\alpha IK}(\beta, \gamma)$ of the 0^+_1 and 0^+_2 states in ^{32}Mg. Dotted curves are contours for negative values.

4.2. Collective wave function and shape fluctuation in neutron-rich isotopes near ^{32}Mg

The nature of the quadrupole collectivity can be examined by analyzing the collective wave function, equation (11), and its distribution in the β–γ plane. An interesting example is neutron-rich Mg isotopes around $A = 32$ [17]. The region of these isotopes is known as an island of inversion, since a large quadrupole collectivity is observed in spite of the neutron magic number $N = 20$. Indeed, a steep change of the energy ratio, $E(4^+_1)/E(2^+_1) = 2.23$, 2.64 and 3.21 in experiment and 2.37, 2.82 and 3.26 in theory for $A = 30$,32 and 34, indicates a dramatic evolution from vibrational to rotational behaviors. The yrare 0^+_2 state is also observed in ^{30,32}Mg, at very low energies close to $E(2^+_1)$. The calculation reproduces well the energies of the yrast 2^+_1 and 4^+_1 states and the yrare 0^+_2 state; they are 0.744, 2.099 and 0.986 MeV in ^{32}Mg, compared with the experimental values 0.885, 2.322 and 1.058 MeV, respectively.

The obtained collective wave function for the ground 0^+_1 state exhibits a clear shape transition from a spherical state in ^{30}Mg (a distribution concentrated around $\beta \sim 0$) to a well deformed state in ^{34}Mg (a distribution around $\beta \sim 0.35$, $\gamma \sim 0$). In ^{32}Mg, the wave function of the ground state indicates a significant fluctuation in the quadrupole shape as it is widely spread over $\beta = 0 \sim 0.4$ along the $\gamma = 0$ line (figure 1(a)). The nature of the 0^+_2 states is also interesting. Experimentally, the 0^+_2 state in ^{32}Mg is populated strongly by the two-neutron transfer (t, p) reaction from ^{30}Mg [1]. It has been argued that the 0^+_1 and 0^+_2 states in ^{30,32}Mg are coexisting states, which are either spherical or deformed, and interchanging with each other across $N = 20$. Our theoretical picture is different. The wave function of the 0^+_2 state is spread over a large interval $\beta = 0 \sim 0.45$, but it has a node around $\beta \sim 0.3$ (figure 2(b)). It indicates a significant shape fluctuation likewise in the ground state, and it contains to some extent a feature of the β-vibration. (The character of the β-vibration in the 0^+_2 state develops well in ^{34}Mg.) This is far from the simple shape coexistence picture.

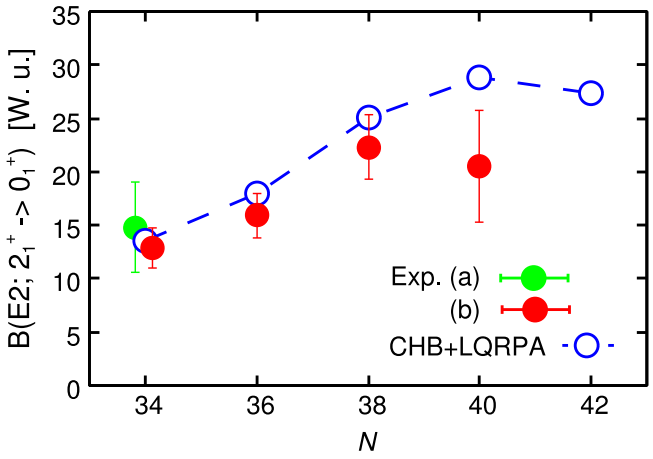

Figure 2. Comparison of theoretical and experimental $B\left(E2; 2_1^+ \rightarrow 0_1^+\right)$ in Weisskopf units for the Cr isotopes. The experimental values are taken from [26–28], while the CHFB +LQRPA value is from [19].

4.3. Shape transition in neutron-rich Cr isotopes

Neutron-rich Cr isotopes with $A \gtrsim 60$ are another example of the new regions of deformation, which is suggested in recent experiments. CHFB calculations using the Skyrme functional (SkM*) for axial deformations indicate that a softening of the deformation potential around $N = 34$ develops further with increasing neutron number, producing a deformed but shallow minimum at $\beta \sim 0.3$ for $N \geqslant 38$ [18, 25]. The calculated excitation energy of the 2_1^+ state decreases gradually with increasing neutron number [19]. The energy ratio $E\left(4_1^+\right)/E\left(2_1^+\right)$ gradually increases from 2.12 at $N = 34$ to 2.68 at $N = 40$, and similarly in $B\left(E2; 2_1^+ \rightarrow 0_1^+\right)$, as shown in figure 2. The isotopic trend of $B\left(E2\right)$ values is in good agreement with the data. The absolute values of the excitation energy are also well described; $E\left(2_1^+\right)$, $E\left(4_1^+\right) = 0.502$, 1.228 MeV in theory versus 0.446, 1.180 MeV in experiment for ^{62}Cr.

From the above quantities one clearly sees the gradual development of quadrupole collectivity. However, the yrast spectra display a transitional behavior between the spherical vibrator and the deformed rotor even in the isotopes with $N = 40$, 42, having the largest collectivity. We can learn more from the collective wave functions. Indeed, we found that the wave functions of the yrast states 0_1^+, 2_1^+, 4_1^+, especially at lower spin members, spread largely from the prolate shape $\beta \sim 0.5$, $\gamma \sim 0$ toward the oblate shape. More significant influence of the γ degrees of freedom is predicted in the yrare $K^\pi = 0^+$ and 2^+ bands in ^{64}Cr.

5. Conclusions and perspectives

The CHFB+LQRPA approach provides us with a scheme to construct the Bohr collective Hamiltonian for the large-amplitude quadrupole shape motion on the basis of the microscopic many-body mean-field dynamics. A great advantage of this approach is that the effect of the velocity-dependent (time-odd) induced field on the inertia of the collective motion, i.e. the Thouless–Valatin effect, is taken into account not only for the rotational moments of inertia but also for the vibrational inertia with respect to the β–γ shape motion. This is achieved by solving the local QRPA equation at each deformation. It seems to solve the problem of the Inglis–Belyaev inertia, that often produces stretched spectra.

Further developments of the CHFB+LQRPA approach are anticipated. We would like to perform calculations on the basis of the selfconsistent Hartree–Fock–Bogoliubov models using a modern energy density functional, for instance the Skyrme functional. Constrained HFB calculations in two-dimensional deformation spaces such as the β–γ plane are numerically intensive, but manageable on reasonable computers. A difficulty lies in the local QRPA part. The QRPA calculation using a realistic density functional requires a large single-particle space to guarantee selfconsistency, allowing, at present, calculations assuming axially symmetric deformations. The QRPA calculation with non-axial deformations will be very tough numerically, and we have to perform the calculations for all the deformations. This is a challenge, but it will become feasible in the near future thanks to the rapid development of computer power. Application to spontaneous fission will then be within scope.

Acknowledgments

This work is supported by KAKENHI (Nos 21340073, 23540294, 23740223 and 25287065).

References

[1] Wimmer K *et al* 2010 *Phys. Rev. Lett.* **105** 252501
[2] Bohr A and Mottelson B R 1975 *Nuclear Structure* vol II (New York: Benjamin)
[3] Ring P and Schuck P 1980 *The Nuclear Many-Body Problem* (Berlin: Springer)
[4] Pomorski K, Kaniowska T, Sobiczewski A and Rohoziński S G 1977 *Nucl. Phys.* A **283** 394
[5] Dudek J, Dudek W, Ruchowska E and Skalski J 1980 *Z. Phys.* A **294** 341
[6] Libert J, Girod M and Delaroche J-P 1999 *Phys. Rev.* C **60** 054301
[7] Próchniak L, Quentin P, Samsoen D and Libert J 2004 *Nucl. Phys.* A **730** 59
[8] Nikšić T, Li Z P, Vretenar D, Próchniak L, Meng J and Ring P 2009 *Phys. Rev.* C **79** 034303
[9] Li Z P, Nikšić T, Vretenar D, Meng J, Lalazissis G A and Ring P 2009 *Phys. Rev.* C **79** 054301
[10] Próchniak L and Rohoziński S G 2009 *J. Phys. G: Nucl. Part. Phys.* **36** 123101
[11] Bertsch G F *et al* 2007 *Phys. Rev. Lett.* **99** 032502
[12] Girod M, Delaroche J-P, Görgen A and Obertelli A 2009 *Phys. Lett.* B **676** 39
[13] Delaroche J-P *et al* 2010 *Phys. Rev.* C **81** 014303
[14] Hinohara N, Sato K, Nakatsukasa T, Matsuo M and Matsuyanagi K 2010 *Phys. Rev.* C **82** 064313

[15] Matsuyanagi K, Matsuo M, Nakatsukasa T, Hinohara N and Sato K 2010 *J. Phys. G: Nucl. Part. Phys.* **37** 064018
[16] Matsuyanagi K, Hinohara N and Sato K 2013 *Fifty Years of Nuclear BCS* ed R A Broglia and K Zelevinsky (Singapore: World Scientific) p 111
[17] Hinohara N, Sato K, Yoshida K, Nakatsukasa T, Matsuo M and Matsuyanagi K 2011 *Phys. Rev.* C **84** 061302(R)
[18] Yoshida K and Hinohara N 2011 *Phys. Rev.* C **83** 061302(R)
[19] Sato K, Hinohara N, Yoshida K, Nakatsukasa T, Matsuo M and Matsuyanagi K 2012 *Phys. Rev.* C **86** 024316
[20] Marumori T, Maskawa T, Sakata F and Kuriyama A 1980 *Prog. Theor. Phys.* **64** 1294
[21] Matsuo M, Nakatsukasa T and Matsuyanagi K 2000 *Prog. Theor. Phys.* **103** 959
[22] Flocard H, Koonin S E and Weiss M S 1980 *Phys. Rev.* C **17** 1682
[23] Negele J W 1982 *Rev. Mod. Phys.* **54** 913
[24] Sakamoto H and Kishimoto T 1990 *Phys. Lett.* B **245** 321
[25] Oba H and Matsuo M 2008 *Prog. Theor. Phys.* **120** 143
[26] Bürger A *et al* 2005 *Phys. Lett.* B **622** 29
[27] Baugher T *et al* 2012 *Phys. Rev.* C **86** 011305(R)
[28] Crawford H L *et al* 2013 *Phys. Rev. Lett.* **110** 242701